이중전압원 분리를 이용한 PMSM의 센서리스 제어

論 文
53B-1-1

A Sensorless PMSM Control Using the Separation of Two Voltage Source

安 珍 雨* · 朴 晟 濬** · 李 東 熙***
(Jin-Woo Ahn·Sung-Jun Park, Dong-Hee Lee)

Abstract - This paper presents a sensorless control strategy of a PMSM(Permanent Magnet Sycchoronous Motor). This method is very simple to compute the position angle of a rotor. A principle and a practical solution are described. A sensorless control algorithm is proposed to remove a mechanical position sensor. The theory is based on the superposition principle. The state equation of a motor is divided into two conditions: one is the state equation of exciting voltage and phase current in a constraint, the other is the state equation of back EMF(Electromotive Force) and phase current in a short circuit. Based on the analysis, short circuit current by back EMF is computed and then the information of position angle is calculated. The proposed method is verified by experimental results.

Key Words : PMSM, superposition, sensorless

1. Introduction

By the extension of modern automated equipments, the use of servomotor in a industrial and a household machines has been on the rapid rise, and the servomotor has been used for the indispensable source of drive in the industrial fields.

Few years ago, most servomotors were to be a DC servomotor, but they have several weaknesses of frequent inspection, repair and limit of high speed operation. However, AC servomotor using permanent magnet has more complicated control scheme than that of DC servomotor, but has advantages over both durability, large ratio of power per weight and torque per current. A permanent magnet synchronous motor(PMSM) has been used in the industrial field also[2~5]. It has a disadvantage such as position detecting device which is to obtain position angle of motor. An encoder and a resolver are generally used to detect rotor's position angle, but these exterior mechanical position sensor has not only a cost disadvantage also problem on reliability by sensor's sudden characteristic change in the worse circumstances. There has been vigorously a study on a sensorless drive for low cost of sensor installation and good robustness on exterior environment.

In this paper, a sensorless control algorithm is proposed to remove a mechanical position sensor[6]. A basic theory is based on the superposition principle. The state equation of a motor is divided into two conditions: one is the state equation of exciting voltage and phase current in a constraint, the other is the state equation of back EMF(Electromotive Force) and phase current in a short circuit. Based on the analysis, short circuit current by back EMF is computed and then obtained the information of position angle is calculated. The proposed method is verified by experimental results.

2. The Modelling of the PMSM

2.1 The Voltage Equation of Motor

The equivalent circuit of 3-phase PMSM with sinusoidal distribution of back EMF is shown in Fig. 1. The voltage, current, and impedance equations obtained from this equivalent circuit as (1).

$$\begin{bmatrix} V_a \\ V_b \\ V_c \end{bmatrix} = \begin{bmatrix} R+pL & 0 & 0 \\ 0 & R+pL & 0 \\ 0 & 0 & R+pL \end{bmatrix} \begin{bmatrix} i_a \\ i_b \\ i_c \end{bmatrix} + \begin{bmatrix} e_a \\ e_b \\ e_c \end{bmatrix} \qquad (1)$$

where $L = l + \frac{3}{2}M$.

Each EMF of (1), e_a, e_b and e_c is represented as each differentiator of flux intercrossed at phase coils. So,

* 正 會 員 : 慶星大學校 電氣電子컴퓨터공학부 敎授·工博
** 正 會 員 : 全南大學校 電氣工學科 助敎授·工博
*** 正 會 員 : OTIS-LG 先任硏究員·工博
接受日字 : 2003년 6월 27일
最終完了 : 2003년 9월 24일

let the maximum value of intercrossing flux λ_a, λ_b and λ_c at phase a, b, and c be λ_m respectively, each representation can be as follows.

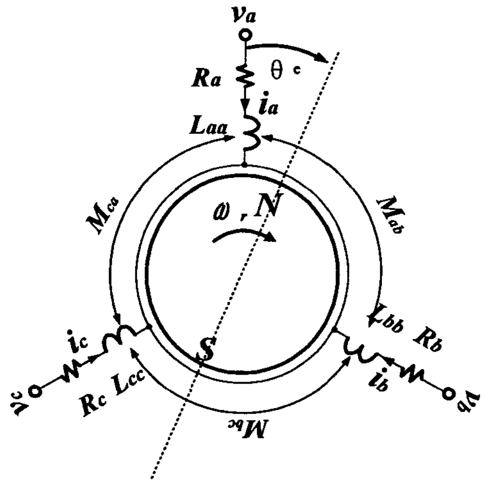

Fig. 1. Three Phase Equivalent circuit of PMSM

$$\lambda_a = \lambda_m \cos(\theta_e)$$
$$\lambda_b = \lambda_m \cos(\theta_e - \frac{2}{3}\pi)$$
$$\lambda_c = \lambda_m \cos(\theta_e + \frac{2}{3}\pi) \quad (2)$$

where θ_e is a clockwise electrical rotor angle with reference to the stator coil at phase a. The inductive EMF obtained from intercrossing flux of phase coil is represented as (3).

$$e_a = \frac{d}{dt}\lambda_a = -\omega_e \lambda_m \sin(\theta_e)$$
$$e_b = \frac{d}{dt}\lambda_b = -\omega_e \lambda_m \sin(\theta_e - \frac{2}{3}\pi)$$
$$e_c = \frac{d}{dt}\lambda_c = -\omega_e \lambda_m \sin(\theta_e + \frac{2}{3}\pi) \quad (3)$$

where ω_e means a rotor's angular velocity and is given as follow.

$$\omega_e = \frac{d}{dt}\theta_e \quad (4)$$

2.2 The Coordinates Transformation of 3-Phase AC Circuit Equation

It is more convenient to represent 2-phase AC than 3-phase in the voltage and current for understanding of 3-phase PMSM characteristic and derivation of control method.

The coordinates need to be transformed for different analysis on motor, and it is called to the coordinates transformation. The transformation matrix from 3-phase AC coordinates(a-b-c) to 2-phase AC coordinates(α-β) can be defined as (5) and this transformation results in the motor's equivalent circuit in the fixed 2 axis α-β coordinates at Fig.2.

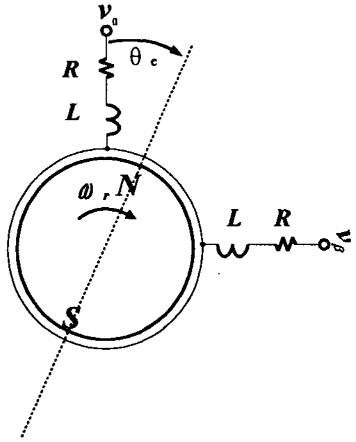

Fig. 2. Two Phase Equivalent circuit of PMSM

$$C = \sqrt{\frac{2}{3}} \begin{bmatrix} 1 & -\frac{1}{2} & -\frac{1}{2} \\ 0 & \frac{\sqrt{3}}{2} & -\frac{\sqrt{3}}{2} \end{bmatrix} \quad (5)$$

The voltage equation of 2-phase equivalent circuit of PMSM in the fixed coordinates is given into (6).

$$\begin{bmatrix} V_\alpha \\ V_\beta \end{bmatrix} = \begin{bmatrix} -R+pL & 0 \\ 0 & -R+pL \end{bmatrix} \begin{bmatrix} i_\alpha \\ i_\beta \end{bmatrix} + \begin{bmatrix} e_\alpha \\ e_\beta \end{bmatrix} \quad (6)$$

This equation can be obtained by multiply the transformation matrix C and the given 3-phase circuit equation together in (1).

where v_α, v_β, i_α, i_β, e_α and e_β are given as follows, respectively.

$$v_\alpha = \sqrt{\frac{2}{3}}\,(v_a - \frac{v_b}{2} - \frac{v_c}{2})$$
$$v_\beta = \frac{(v_b - v_c)}{\sqrt{2}} \quad (7)$$

$$i_\alpha = \sqrt{\frac{2}{3}}\,(i_a - \frac{i_b}{2} - \frac{i_c}{2})$$
$$i_\beta = \frac{(i_b - i_c)}{\sqrt{2}} \quad (8)$$

$$e_\alpha = -\sqrt{\frac{3}{2}}\,\omega_e \lambda_m \sin(\theta_e)$$
$$e_\beta = \sqrt{\frac{3}{2}}\,\omega_e \lambda_m \cos(\theta_e) \quad (9)$$

If (6) obtained from the 2-axis fixed coordinates(α-β) is rearranged and also represented into the state equation of PMSM, (14) can be given as follows

$$\begin{bmatrix} i_\alpha \\ i_\beta \end{bmatrix} = \begin{bmatrix} -\frac{R}{L} & 0 \\ 0 & -\frac{R}{L} \end{bmatrix} \begin{bmatrix} i_\alpha \\ i_\beta \end{bmatrix} + \frac{1}{L}\begin{bmatrix} v_\alpha \\ v_\beta \end{bmatrix} + \frac{1}{L}\begin{bmatrix} e_\alpha \\ e_\beta \end{bmatrix} \quad (10)$$

And the torque equation is given in (11).

$$T_e = p_{poles} \cdot \lambda_m(-i_\alpha \sin\delta + i_\beta \cos\delta) \tag{11}$$

where stands for the angle between rotor and stator.

2.3 The Principle of Sensorless PMSM using Superposition Principle

The voltage equation of PMSM given in 2-phase AC coordinates α-β can be represented into the equivalent circuit in the 2 fixed reference axis (α-β) in Fig. 3 and from (6).

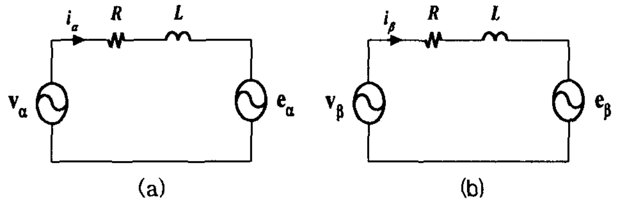

Fig. 3. Equivalent circuit of PMSM by α-β axis
(a) Equivalent circuit of α axis
(b) Equivalent circuit of β axis

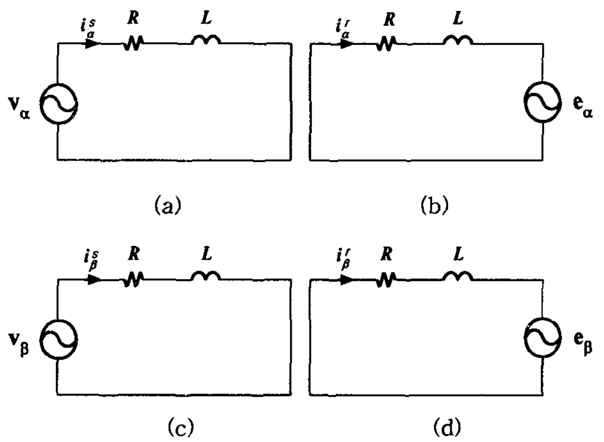

Fig. 4. Equivalent circuit of PMSM using superposition principle
(a) Equivalent circuit of α axis terminal voltage
(b) Equivalent circuit of α axis back EMF voltage
(c) Equivalent circuit of β axis terminal voltage
(d) Equivalent circuit of β axis back EMF voltage

As you can see in the circuit of α-β coordinates in Fig. 3, the sources *forming the motor current are a back* EMF voltage and a terminal voltage as two voltage sources. Accordingly, the use of superposition principle which separates into two voltage source can be represented into the equivalent circuit in Fig. 4.

According to Fig. 4, the source of current can be expressed the inductive EMF term occurred by the phase voltage from inverter and the motor's rotation. The motor current becomes a indispensable factor for overcurrent detection and excellent velocity control of motor. If the motor parameters R and L can be known, the current component by the phase voltage induced from inverter can be found easily. In the equivalent circuit of Fig. 4, the circuit represented with the inductive EMF by the motor's rotation and the phase voltage from inverter can be obtained into the following state equation.

$$\begin{bmatrix} \dot{i}_\alpha^s \\ \dot{i}_\beta^s \end{bmatrix} = \begin{bmatrix} -\frac{R}{L} & 0 \\ 0 & -\frac{R}{L} \end{bmatrix} \begin{bmatrix} i_\alpha^s \\ i_\beta^s \end{bmatrix} + \frac{1}{L} \begin{bmatrix} v_\alpha \\ v_\beta \end{bmatrix} \tag{12}$$

$$\begin{bmatrix} \dot{i}_\alpha^r \\ \dot{i}_\beta^r \end{bmatrix} = \begin{bmatrix} -\frac{R}{L} & 0 \\ 0 & -\frac{R}{L} \end{bmatrix} \begin{bmatrix} i_\alpha^r \\ i_\beta^r \end{bmatrix} + \frac{1}{L} \begin{bmatrix} e_\alpha \\ e_\beta \end{bmatrix} \tag{13}$$

The current term by the back EMF can be computed by the difference between the detected real motor current and the current by the phase voltage. Therefore, the current component can be easily obtained, and then this current component of back EMF comes to be directly controlled by the voltage of back EMF. The current term of back EMF, i.e., becomes physical quantity passed through a low-pass filter.

So, the back EMF can be theoretically computed by passing the back EMF's current through high-pass filter, but it needs some techniques for dealing with high-pass filter with weakness at noise. In order to verify back EMF from the current component by back EMF, you can see (13) including the differential term, but come to know that the back EMF term in this equation has lots of switching noise. It is necessary to compute back EMF from numerical solutions of state equation for solving this noise problem. The complete solution of α-axis back EMF in the state equation of (13) is given as follow.

$$i_\alpha^r(t) = \frac{e_\alpha}{R}(1 - e^{-\frac{R}{L}t}) + i_\alpha^r(0)e^{-\frac{R}{L}t} \tag{14}$$

This solution can be represented into the discrete form as (15).

$$i_\alpha^r(n) \Box \frac{e(n)}{R}(1 - e^{-\frac{R}{L}\Delta T}) + i_\alpha^r(n-1)e^{-\frac{R}{L}\Delta T} \tag{15}$$

If motor parameter and sampling time are determined, the exponential term of (14) can be dealt with the constant, and its value can be defined as follow.

$$K_T \Box e^{-\frac{R}{L}\Delta T} \tag{16}$$

Thus, the back EMF term from (15) and (16) can be given as follow.

$$e_\alpha(n)=\frac{R}{(1-K_T)}\left[i_\alpha^r(k)-K_T i_\alpha^r(n-1)\right] \tag{17}$$

The solution for back EMF on β-axis can be solved as mentioned above, and if the back EMF can be given on α-β axis, the electrical position angle of rotor can be following

$$\theta_e=\tan^{-1}\frac{e_\alpha}{e_\beta}\ . \tag{18}$$

The equation obtained from (18), strictly speaking, is also equal to that which passed through high-pass filter. Hence, a simple prediction method is used to remove appropriately the noise component of electrical position angle, and its schematic diagram cab be illustrated in Fig. 5, where Z^{-1} means the delay term. The $\theta_{e(k)}$ is represented into the discrete form as (18).

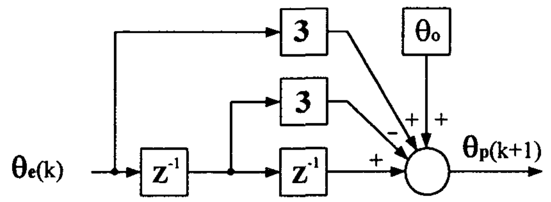

Fig. 5. Schematic diagram of quadratic position prediction

The block diagram of Fig. 5 can be numerically expressed as follow, where θp(K+1) means the prediction value from position angle computed by back EMF to the position angle in the next sampling, where θ0 means an initial position angle at a start.

$$\theta_p(k+1) = 3[\theta_e(k)-\theta_e(k-1)] + \theta_e(k-2)+\theta_o \tag{19}$$

The estimation of rotor position angle can be estimated in this method without reference to a back EMF constant, but the back EMF constant is needed to estimate the motor speed. If the back EMF on α-β axis is given, the electrical angular velocity of rotor can be given as follow.

$$\omega_e = \frac{1}{K_E}\sqrt{e_\alpha^2+e_\beta^2} \tag{20}$$

where K_E stands for the back EMF constant.

The information on the number of motor poles is necessary to find mechanical angular velocity from electrical angular velocity. The relation of electrical and mechanical angle according to the number of motor pole can be given as follow.

$$\omega_r = \frac{\omega_e}{p_{poles}} \tag{21}$$

where p_{poles} means the motor pole pair.

2.4 The Structure of Controller

If transformed from 3-phase stationary coordinates to 2-phase stationary coordinates(α-β) in controlling PMSM, and then the latter transformed into 2-phase rotating coordinates(d-q), all values of variables come to be DC, and also their characteristic to be the same form of DC motor, which makes a control simple. The transformation and inverse transformation from 3-phase stationary coordinates to 2-phase stationary coordinates (α-β) are as followings.

$$\begin{bmatrix} f_q^s \\ f_d^s \\ f_o^s \end{bmatrix} = \frac{2}{3}\begin{bmatrix} 0 & \frac{\sqrt{3}}{2} & -\frac{\sqrt{3}}{2} \\ 1 & -\frac{1}{2} & -\frac{1}{2} \\ \frac{1}{2} & \frac{1}{2} & \frac{1}{2} \end{bmatrix}\begin{bmatrix} f_a \\ f_b \\ f_c \end{bmatrix} \tag{22}$$

$$\begin{bmatrix} f_q^s \\ f_d^s \end{bmatrix} = \begin{bmatrix} 0 & \frac{1}{\sqrt{3}} & -\frac{1}{\sqrt{3}} \\ \frac{2}{3} & -\frac{1}{3} & -\frac{1}{3} \end{bmatrix}\begin{bmatrix} f_a \\ f_b \\ f_c \end{bmatrix} \tag{23}$$

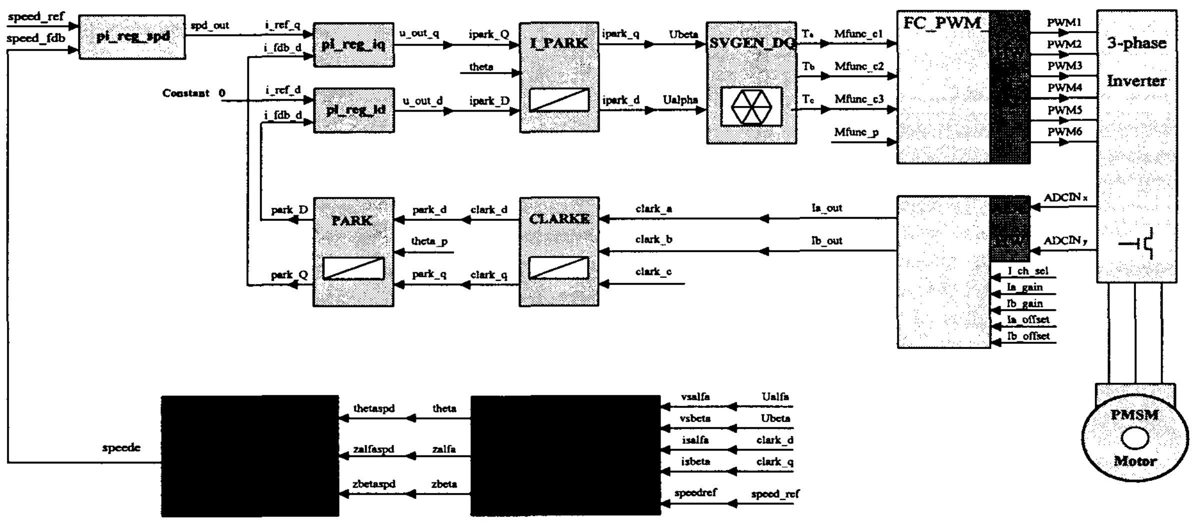

Fig. 6. Diagram of controller

The transformation and inverse transformation from 2-phase stationary coordinates to 2-phase rotating coordinates(d-q) are as followings.

$$\begin{bmatrix} f_q^r \\ f_d^r \end{bmatrix} = \begin{bmatrix} \cos\theta & -\sin\theta \\ \sin\theta & \cos\theta \end{bmatrix} \begin{bmatrix} f_q^s \\ f_d^s \end{bmatrix} \quad (24)$$

$$\begin{bmatrix} f_q^s \\ f_d^s \end{bmatrix} = \begin{bmatrix} \cos\theta & \sin\theta \\ -\sin\theta & \cos\theta \end{bmatrix} \begin{bmatrix} f_q^r \\ f_d^r \end{bmatrix} \quad (25)$$

Fig. 6 shows the overall block diagram of proposed algorithm. A SVPWM(space vector pulse width modulation) in the block diagram uses VSI(voltage source inverter), and the space vector modulation technique is applied in the modulation method. Every algorithm except inverter is also constructed into software to reduce a hardwares. The sampling time is 200μsec in this algorithm.

There are DC-LINK voltage and phase current as inputs to realize this algorithm. After transforming the 3-phase stationary coordinates into 2-phase stationary coordinates by using these inputs, first the rotor position angle and velocity is estimated and then converted into 2-phase rotating coordinates for control.

3. Experimental Results and Analysis

Fig. 7(a) shows the rotor of motor for a washing machine, and Figure 7(b) shows the stator of motor. As you can see in the figure, motor with 48 poles is designed for a low speed.

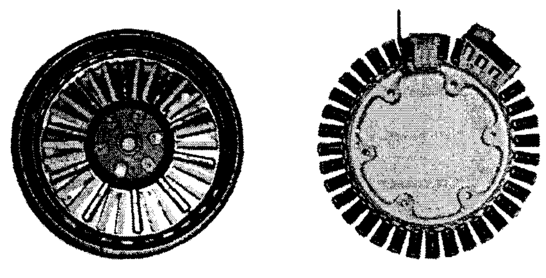

(a) (b)

Fig. 7. PMSM configurations
(a) Rotor (b) Stator

Fig. 8 shows the measured back EMF waveforms of PMSM into a washing machine, where it can be found that this back EMF has sine waves.

Fig. 9 illustrates the relation between rotation speed and back EMF in varying rotating speed of motor. It can be, as you can see in Fig. 9, found that the ratio value of back EMF to speed has nearly a linearity over 98 %. Therefore, the speed can be easily solved by multiplying

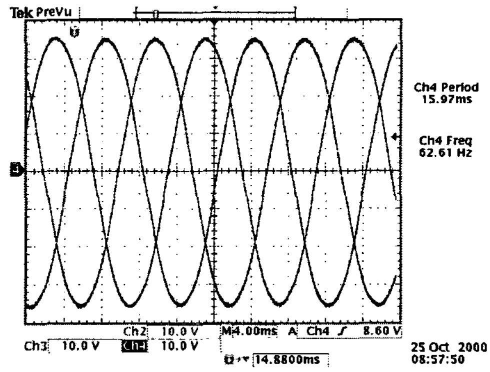

Fig. 8. Back EMF waveforms of phase a, b and c

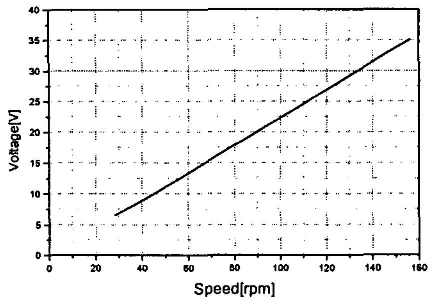

Fig. 9. Back EMF of PMSM

the back EMF constant, if the back EMF is to be computed. When DC voltage 24V is applied, moreover, forced to measure resistance R and inductance L as important parameters for sensorless control, the current waveform is shown in Fig. 10. The values of R and L can be found by analyzing the rise curve of the current waveform at each phase of motor in Fig. 10.

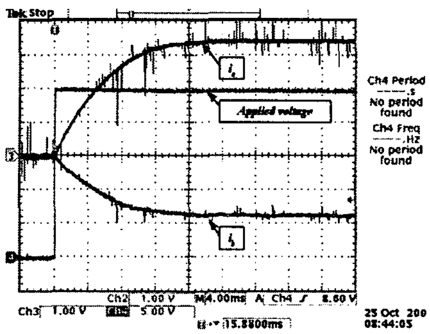

Fig. 10. Current waveform at step change of DC voltage

This experiments are accomplished with the measured parameters in Table 1.

Table 1. The measured parameters

Winding resistance	1.981[Ω]
Winding inductance	10.8[mH]
EMF contantant	0.224[rpm/V]
Number of poles	24 poles
Rated current	6.0[A]
Rated Speed	600[rpm]

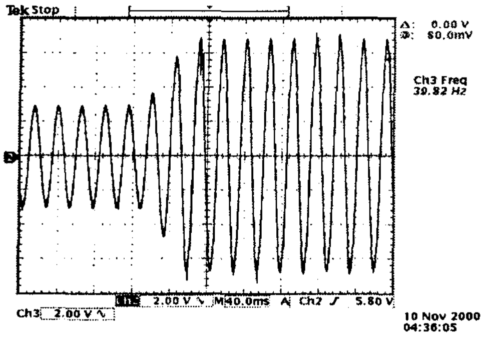

Fig. 11. Real and estimated current

Fig. 11 shows the waveform comparing the solution of state equation in (12) with real current by changing the terminal voltage in a motor constraint. The back EMF is equal to zero in order to verify R and L measured in the above.

In the figure, it can be known that it estimates almost perfectly to the real current with all the changes of input voltage. It shows that the value of R and L among the motor parameters are accurate.

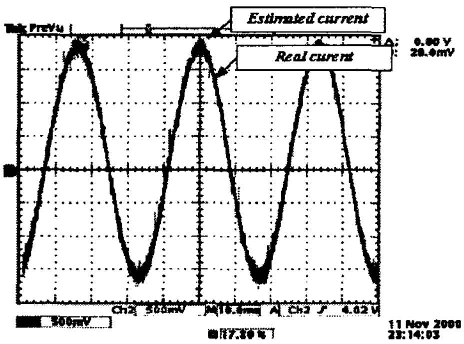

Fig. 12. Real and estimated current (in a short circuit condition)

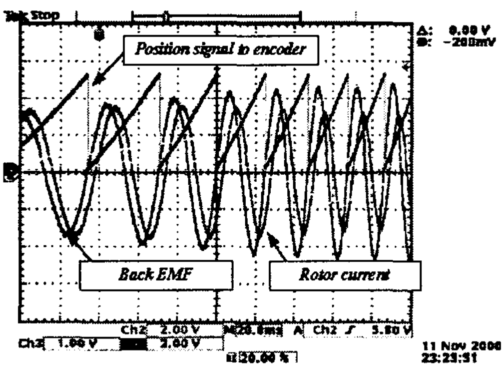

Fig. 13. Rotor current, back EMF and position signal of rotor

When making a short at the motor terminal, and then driving the motor with exterior power, the motor current and the estimated current are shown in Fig. 12. The terminal current, the estimated back EMF and the electrical rotor position detected from encoder are shown in Fig. 13. It can be, as you can see in Fig. 13, known that it can estimate a position with coincidence in α-axis back EMF and the zero point of rotor.

Fig. 14 shows the Real current, the estimated current and the estimated speed with the same condition in Fig.13.

Fig. 15 shows real rotor position and the estimated rotor position when the sensorless control is achieved by the proposed algorithm. It can be found that the estimation value of rotor position is almost same as that of real one.

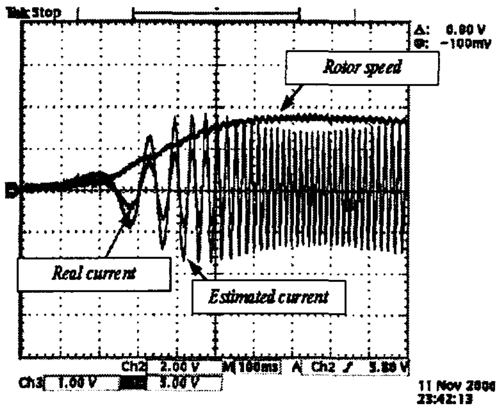

Fig. 14. Real and estimate current at external starting

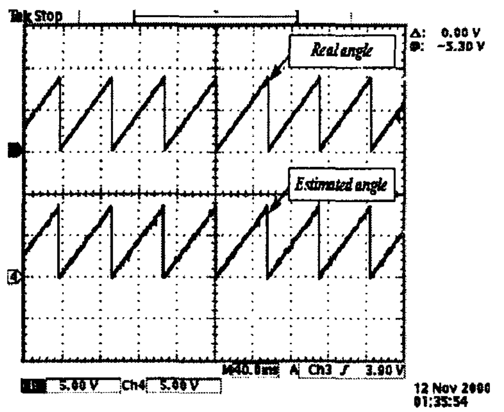

Fig. 15. Real and estimated angle

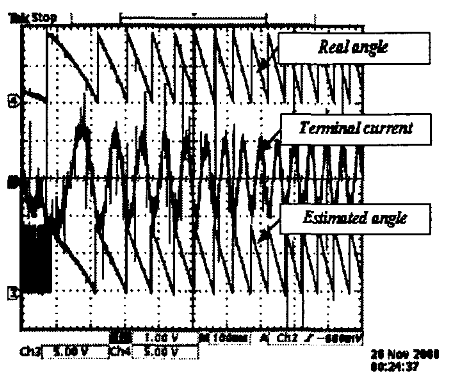

Fig. 16. Real and estimated angle at a starting (Terminal current, estimated angle and real angle from top trace)

Fig. 16 shows the terminal current, the estimated and the real angle during sensorless control at initial angle difference 45°. Since a cylindrical PMSM has a constant inductance regardless of the rotor position, no information can be obtained about the initial position. Therefore, it moves with the zero initial position and then its mobile characteristic is somewhat changed by the initial position of rotor. The stability of proposed control algorithm get within initial angle difference 74° from the experimental results.

4. Conclusions

In this paper, a method of sensorless control algorithm based on superposition principle is proposed. They are analysed after the state equation of motor is separated into two state equations in each constraint and short circuit. Based on this analysis, the back EMF component can be analysed by simply computing the short circuit current by back EMF component and a position angle computation technique is proposed. The experiment using a PMSM with a washing machine is excuted to verify a properness of control algorithm and then results in the following characteristics.

1. In this control algorithm, the rotor position can be estimated without an information about back EMF constant.
2. Even if R and L values vary up to 30%, a stable sensorless control is possible.
3. The characteristic can be changed somewhat by the initial rotor position at a start.

When the rotor position is aligned to fix the initial position, the alignment characteristic can be changed by the rotor position.

If this control algorithm is applied to the PMSM, an improvement in productivity and an increase on durability are expected by not only the performance improvement of products but also the simple structure. In addition, even though a motor characteristic or a manufacture is changed, the changed system can be accessed by using the known motor parameters.

References

[1] T. M. Jahns, "Torque Production in Permanent Magnet Synchronous Motor Drives with Rectangular Current Excitation", IEEE Trans. Indust. Applicat., Vol. 20, No. 4, pp. 803-813, July/June 1984.

[2] H. R. Bolton and R. A. Ashen, "Influence of Motor Design and Feed-current Waveform on Torque Ripple in Brushless DC Drive", Proc. of IEE, Vol. 131, Part B, No. 3, pp. 82-90, May 1984.

[3] D. Hanselman, J. Y. Hung and M. Keshura, "Torque ripple analysis in brushless permanent magnet motor drive", Proc. of ICEM 92, Manchester, UK, pp. 823-827, Sept. 1992.

[4] H. Le-Huy, R. Perret and R. Feuillet, "Minimization of Torque Ripple in Brushless DC Motor Drive", IEEE Trans. Indust. Applicat., Vol. 22, No. 4, pp. 748-755, July/Aug. 1986.

[5] J. Y. Hung and Z. Ding, "Minimization of Torque Ripple in Permanent Magnet Motors", Proc. 18th IEEE Industrial Electronics Conf., San Diego, CA, pp. 459-463, Nov. 1992.

[6] J. W. Ahn, et al "A High Performance Sensorless Speed Control Scheme of PMSM with Time Compression Method", Proc. of Korea-Japan Symp. pp. 98-102, Oct. 2002.

저 자 소 개

안 진 우 (安 珍 雨)

1958년생. 1984년 부산대 전기공학과 졸업. 1986년 동 대학원 전기공학과 졸업(석사). 1992년 동 대학원 전기공학과 졸업(박사). 1995년 12월~1996년 2월 영국 글래스고우대 방문연구원. 1998년 8월~1999년 8월 미국 위스컨신대 방문교수. 1992년~현재 경성대 전기전자컴퓨터공학부 교수.

박 성 준 (朴 晟 濬)

1965년생. 1991년 부산대 전기공학과 졸업. 1996년 동 대학원 졸업(박사). 1996년~2000년 거제대학 조교수. 2001년~2003년 8월 동명대 전기자동화계열 조교수. 2003년 9월~현재 전남대 전기공학과 조교수.

이 동 희 (李 東 熙)

1970년 생. 부산대학교 전기공학과졸업. 2001년 동 대학원 전기공학과 졸업(공학박사) 2002~현재 OTIS-L선임연구원

Tel : +82-51-522-1503

e-mail : dhlee5@hanmail.net